SLAC-PUB-14367

A Low-Charge, Hard X-Ray FEL Driven with an X-band Injector and Accelerator

Yipeng Sun, Chris Adolphsen, Cecile Limborg-Deprey,
Tor Raubenheimer and Juhao Wu
SLAC National Accelerator Laboratory, Menlo Park, California 94025, USA

February 9, 2012

Abstract

After the successful operation of FLASH (Free-Electron Laser in Hamburg) and LCLS (Linac Coherent Light Source), soft and hard X-ray Free Electron Lasers (FELs) are being built, designed or proposed at many accelerator laboratories. Acceleration employing lower frequency RF cavities, ranging from L-band to C-band, is usually adopted in these designs. In the first stage bunch compression, higher-frequency harmonic RF system is employed to linearize the beam's longitudinal phase space, which is nonlinearly chirped during the lower frequency RF acceleration process. In this paper, a hard X-ray FEL design using an all X-band accelerator at 11.424 GHz (from photo-cathod RF gun to linac end) is presented, without the assistance of any harmonic RF linearization. It achieves LCLS-like performance at low charge using X-band linac drivers, which is more versatile, efficient and compact than ones using S-band or C-band rf technology. It employs initially 42 microns long (RMS), low charge (10 pC) electron bunches from an X-band photoinjector. An overall bunch compression ratio of roughly 100 times is proposed in a two stage bunch compressor system. The start-to-end macro-particle 3-D simulation employing several computer codes is presented in this paper, where space charge, wakefields, incoherent and coherent synchrotron radiation (ISR and CSR) effects are included. Employing an undulator with a short period of 1.5 cm, a Genesis FEL simulation shows successful lasing at a wavelength of 0.15 nm with a pulse length of 2 fs and a power saturation length as short as 20 meters, which is equivalent to LCLS low charge mode. Its overall length of both accelerators and undulators is 180 meters (much shorter than the effective LCLS overall length of 1230 meters, including an accelerator length of 1100 meters and an undulator length of 130 meters), which makes it possible to be built in places where only limited space is available.

1 Overview

A laser (Light Amplification by Stimulated Emission of Radiation) is a device that emits light with high degree of spatial and temporal coherence. Unlike conventional lasers, Free Electron Lasers (FELs) use the lasing of relativistic electron beam traveling through a magnetic undulator, which

Submitted to Physical Review Special Topics - Accelerators and Beams
Work supported in part by US Department of Energy contract DE-AC02-76SF00515.

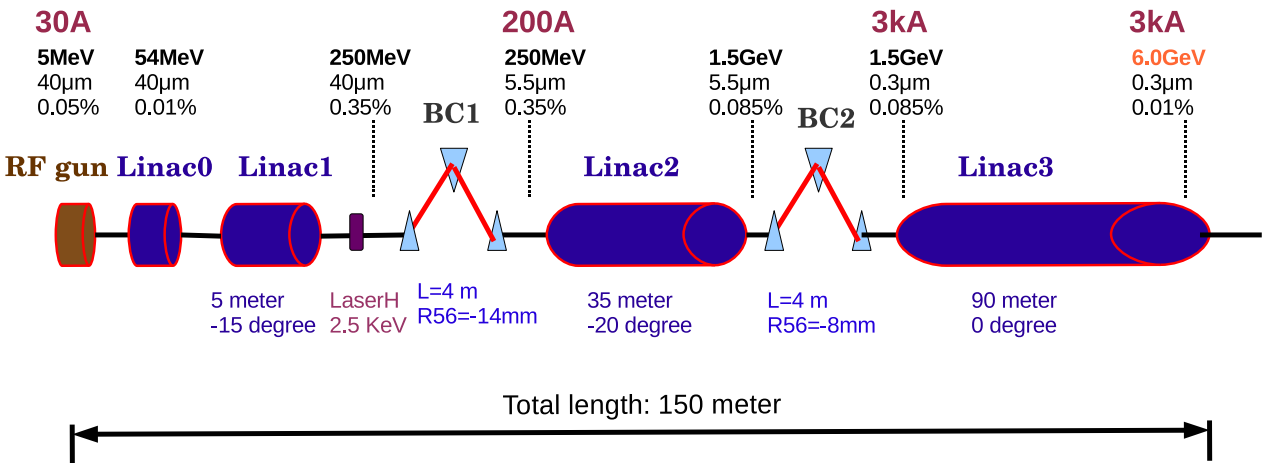

Figure 1: Sketch of a compact (150 m) hard X-ray FEL driver using all X-band accelerators, from X-band photoinjector to X-band linac end. An average 'real estate' acceleration gradient of 60 MV/m is assumed in the X-band accelerator structures, and two stage bunch compression system is adopted with relatively weak dipole magnets to suppress ISR and CSR effects. The linac for the hard X-ray FEL design has a final electron bunch energy of 6 GeV with a peak current of 3 kA, while the soft X-ray FEL design has 2 GeV, 1 kA electron bunches. A final pulse duration length of 2 fs to 6 fs is achieved with a bunch charge of 10 pC. The slice energy spread is between $0.01\% - 0.02\%$, and the slice normalized transverse emittance is below 0.2 μm.

can reach high power and can be widely tunable in wavelength (electron beam energy). It was proposed by J. Madey and demonstrated for the first time at Stanford University in 1970s [1] [2], where a 24 MeV electron beam and 5 meters long wiggler were used. In this experiment, the lasing happened with an oscillator configuration. Since then, the radiation wavelength has been pushed downwards with higher beam energy and shorter undulator period available. Lacking mirrors with good reflectivity for shorter and shorter radiation wavelength, researchers improve the electron bunch qualities so that the lasing can happen based on a collective instability mechanism within a single path for the electrons traversing the undulator. This is the so-called Self-Amplified Spontaneous Emission (SASE) operation mode of an FEL [3, 4, 5]. Recently there are several FELs being operated, constructed or proposed [6] [7] [8] in the X-ray wavelength range. The two currently operating X-ray FEL facilities, FLASH (Free-Electron Laser in Hamburg) in Germany and LCLS (Linac Coherent Light Source) in the United States, both work under Self-Amplified Spontaneous Emission (SASE) mechanism, which does not require external seeding (modulation) or mirrors.

FLASH is the world's first X-ray FEL and has been open to the photon science user community since 2005. It has a maximum beam energy of 1.2 GeV and can deliver 10-70 fs long FWHM photon pulses in a wavelength range of 44 nm to 4.1 nm [6]. The linac is 150 m long and consists of L-band (1.3 GHz) superconducting RF cavities that can accelerate multi-bunch beams at a 'real estate' gradient of 15 MV/m on average. The peak bunch current is increased from 50-80 A to 1-2 kA through two stage bunch compression, with a bunch charge between 0.5 nC and 1 nC. Due

to the nonlinear energy chirp associated with the long (7 ps rms) initial bunch length, there is a sharp spike in the final bunch longitudinal distribution as this part is compressed more than the other parts. Consequently, only the small portion of the charge in this sharp spike can radiate and saturate in the undulator. Recently, a 3.9 GHz harmonic RF module was installed before the first bunch compressor to linearize the bunch energy correlation, which produces a more uniform bunch compression in the first stage and thus improves its X-ray FEL performance.

LCLS is now in routine operation, providing soft and hard X-rays to its users with good spatial coherence at wavelengths from 2.2 nm to 0.12 nm by varying the bunch energy from 3.5 GeV to 15 GeV [7]. Single bunch electron beam acceleration is achieved with S-band (2.856 GHz) accelerator structures operating at average 'real estate' gradients of about 17 MV/m. The linac length is roughly 1 km long and includes two stages of bunch compression. Similar to the linearization scheme adopted at FLASH, a fourth harmonic RF linearizer is employed at LCLS, in this case using a 0.6 m long X-band (11.4 GHz) structure that had been developed for NLC. Also, a laser heater is used to increase the uncorrelated energy spread, which provides more Landau damping and suppresses beam collective effects, such as the space charge effect induced microbunching instability. The machine can operate with either a high (250 pC), or low (20 pC) bunch charge and achieve a final peak bunch current of 3 kA in either case. With a slice transverse emittance around 0.6 μm and a slice energy spread around 0.01-0.02%, usually X-ray radiation achieves saturation within 60 meters.

Newer XFELs (at Spring8 and PSI) [8] use C-band (5.7 GHz) normal-conducting linac drivers, which can sustain higher acceleration gradients, and hence shorten the linac length, which are more efficient at converting RF energy to bunch energy. The X-band (11.4 GHz) RF technology developed for NLC/GLC offers even higher gradients and efficiencies, and the shorter RF wavelength allows more versatility in longitudinal bunch phase space compression and manipulation.

In this paper, a 6 GeV hard X-ray FEL design is described that has a compact (150 m) X-band injector and linac and a 30 m undulator, which can radiate at a wavelength of 0.15 nm. A sketch of the accelerator system is shown in Fig. 1. The 'real estate' acceleration gradient and 'active' RF cavity length of each linac section are summarized in Table 1. It would operate in the short bunch length, low charge regime, which guarantees a small nonlinear energy correlation along the bunch from the X-band acceleration, where the RF wavelength is 26 mm. No harmonic RF linearization is necessary in either stage of bunch compression, as the employed initial bunch length is short enough with respect to the RF wavelength [9]. An average acceleration gradient of 80 MV/m is assumed, which has been achieved routinely in the SLAC NLCTA X-band linac. It produces an effective average 'real estate' gradient of 60 MV/m when components such as quadrupoles are included. A two stage bunch compression system is adopted, where two normal four-dipole chicanes are carefully designed as the bunch compressors. The electron bunch generated by the X-band photoinjector has a low charge of 10 pC, an rms length of 42 μm and a peak current of 30 A. This electron bunch is compressed to a final length of 0.9-0.3 μm rms and a peak current of 1-3 kA in two stages. A laser heater is located before the first stage of bunch compression to increase the un-correlated energy spread, which provides more Landau damping to suppress beam collective effects such as the space charge effect induced microbunching instability. The final electron beam energy can be tuned in the range of 2-6 GeV depending on the desired X-ray photon energy. Soft X-ray FEL operation at bunch energies below 6 GeV is not presented in this paper as the beam dynamics is less challenging in that case.

Table 1: RF parameters of each linac.

	Linac1	Linac2	Linac3
'real estate' gradient [MV/m]	57	54	60
'active' RF length [m]	2.6	17	56

The following sections discuss the X-band photoinjector design and simulation studies, the overall FEL accelerator design configuration, the accelerator optics, X-band wakefield calculations and impacts, start-to-end 3-D simulation results, timing jitter sensitivity, misalignment and FEL simulation with GENESIS [10].

2 X-band photoinjector

The initial electron beam is produced in an X-band photoinjector. This photoinjector consists of a 5.59 cell gun running with an RF peak field of 200 MV/m on the cathode. This gun is presently being fabricated and is going to be tested at the X-band gun test area of the NLCTA at SLAC [11].

Table 2: ASTRA simulation results, optimized for 3 different initial laser profiles.

Q [pC]	r[mm]	$\epsilon_{x,100\%}/\epsilon_{x,95\%}$ [mm-mrad]	σ_z [μm]	$Q/\sigma_z/\epsilon_x/1000$ [C/m^2/rad]
10	0.1	0.070/0.052	105	1.83
10	0.2	0.092/0.076	55	2.39
10	0.3	0.140/0.118	42	2.01

A first generation of this gun had been commissioned in 2006 for a Compton scattering experiment [12]. It was demonstrated that a 200 MV/m peak field can be sustained with no breakdown and manageable dark current. Given the high peak field of 200 MV/m and thanks to the short wavelength, the electron beam is very rapidly accelerated to ultrarelativistic energies in this X-band gun. After 1mm, the Lorentz beta coefficient is 0.4 in this X-band gun, against a value of 0.2 at the same location in the LCLS S-band gun. As a consequence, shorter bunch lengths can be obtained. Simulations were carried out with the computer code ASTRA [13], where the initial distribution of the laser has a longitudinal gaussian profile with a FWHM length of 100 fs.

The photo-emission is thus that of a "blow-out" regime [14], which linearizes at best the longitudinal phase space of the photo-electrons. In the ASTRA simulations the initial transverse distribution at the cathode is a uniform disk. The optimum transverse profile in the "blow-out" regime, which leads to a perfect ellipsoid with uniform space charge density, has a radial function distribution represented by a half-circle as described by equation (6) of reference [14]. A truncated gaussian distribution could be used as it approaches better the half-circle than the uniform one and as it is easier to produce experimentally. However the purpose of this paper is not to study the "blow-out" regime in details. Optimization of the optics to minimize the transverse emittance was done for three different sets of initial spot size radii. In general, the trade-off is made in balancing space charge effects in the transverse and longitudinal planes, or in other words, between choosing bunch length, energy spread and transverse emittance.

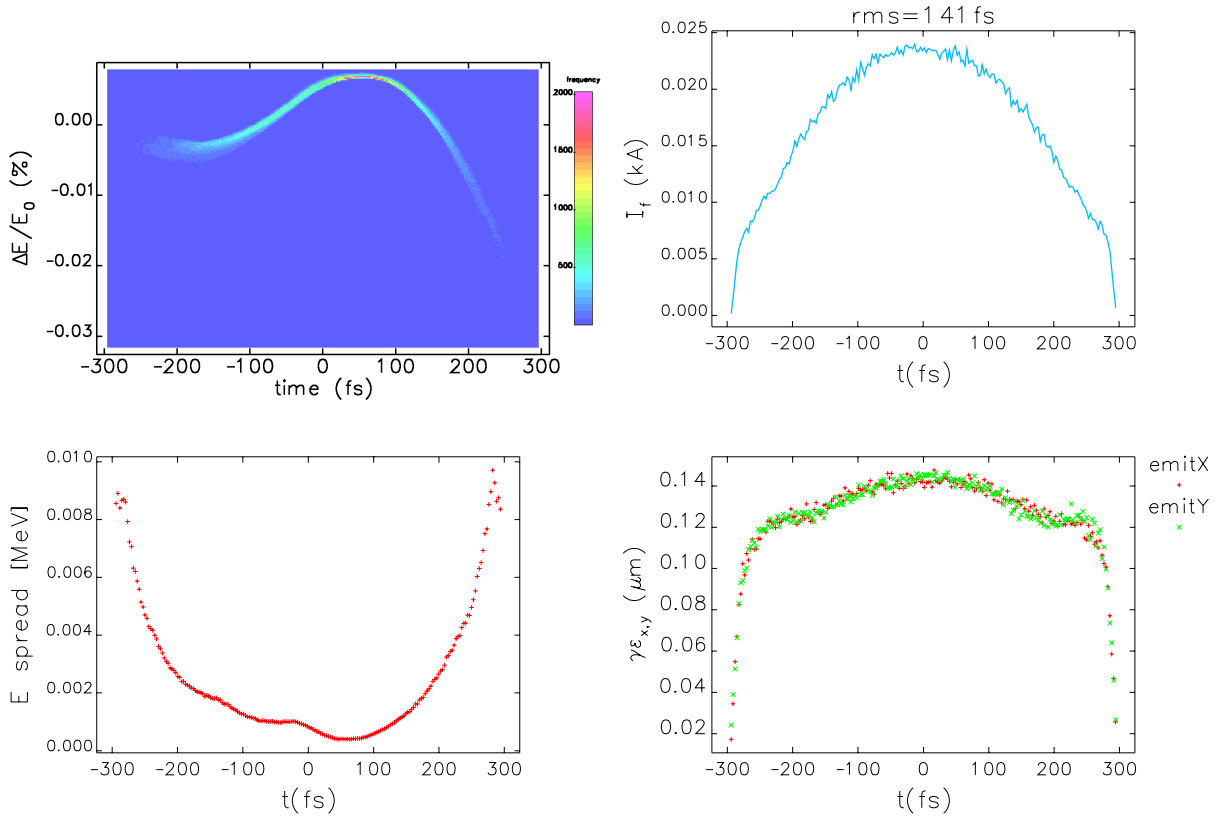

Figure 2: Electron beam properties at the end of Linac0 (see Fig. 1), with a beam energy of 54 MeV. Left top: longitudinal phase space; left bottom: longitudinally sliced energy spread; right top: current profile; right bottom: longitudinally sliced emittance. A normalized transverse emittance of 0.14μm is achieved for a bunch charge of 10 pC, with an RMS bunch length of 42μm. The longitudinal distribution of this electron bunch follows a hyperbolic shape, with a relative slice energy spread of 2×10^{-5}.

The distribution used in the start-to-end simulations was the one having a 0.3 mm radius and a shortest bunch length, which provides a most linear bunch compression process afterwards. This configuration gives a 42 μm rms bunch length after acceleration to a beam energy of 54 MeV, which optimization result corresponds to the one providing a higher peak brightness as shown in the fifth column of Table 2. The thermal emittance used in the simulations is based on the measured LCLS thermal emittance of 0.9 mm mrad per mm radius, which is twice the theoretical value of the commonly accepted model. The longitudinal phase space, longitudinally sliced energy spread and transverse emittance of the electron bunch, associated with the electron bunch current profile are shown in Fig. 2, at the end of Linac0 (see Fig. 1) where the electron beam energy is 54 MeV. This output data file from ASTRA denotes an electron bunch with a half million macro-particles, and it is taken as an initial bunch distribution in the subsequent simulations.

3 X-band linac and bunch compression

LiTrack [15] 1-D simulation is performed at a first place, to approximately evaluate the required RF and bunch compressor parameters, such as RF phase and linac length, beam energy at two bunch compressors, longitudinal dispersion R_{56} of these two bunch compressors. In detail, a beam energy of 250 MeV is chosen for bunch compressor one, which is the same as LCLS and is a compromise between balancing space charge impacts and maintaining necessary un-correlated relative energy spread, in order to minimize CSR induced energy change by Landau damping. Given a total final beam energy of 6 GeV, a reasonable beam energy between 1 GeV and 2 GeV should be adopted at bunch compressor two. While the upper limit is from a design final beam energy, ISR in the bends and ability to de-chirp in Linac3, the lower limit is mainly set by the timing jitter tolerance associated with the wakefield cancellation scheme which will be discussed in Sec. 3.4. The RF phase (relative to crest) is chosen to be as large as possible, so the final bunch length is less sensitive to timing jitter, also one then only needs a smaller longitudinal dispersion R_{56} in the bunch compressors given a same required bunch compression ratio. In general these two choices both result in a more linear bunch compression process [9]. However, a large RF phase also introduces a less efficient linac and larger dispersive emittance dilution associated with a larger energy spread. After choosing basic parameters from longitudinal 1-D simulation studies, in a next step one needs to design accelerator optics and perform 3-D start-to-end simulation with all the collective effects to evaluate the performance of the FEL design.

The X-band linac acceleration and bunch compression starts at an arbitrary beam energy of 54 MeV, by taking an output from ASTRA which simulates 3-D bunch motion from laser interaction on the target and includes collective effects such as space charge. The ASTRA output bunch distribution, as shown in Fig. 2, is matched to the optics of Linac1 using four quadrupoles. The detailed optics design, X-band wakefields, bunch compression and phase space manipulation, timing jitter and misalignment impacts are presented in the following subsections.

3.1 Optics design

As stated above, an output bunch distribution at 54 MeV is taken as an input for the 3-D simulation through the whole linac. It is matched to the periodic FODO cell of Linac1 using four independent

quadrupole magnets. All the matching work is done in the accelerator design code MAD8 [16]. The basic X-band RF acceleration cell is based on FODO focusing structure, with both horizontal and vertical betatron phase advance equalling 72 degree per cell. The consideration on choosing a proper average beta function, or equivalently a proper periodic FODO cell length, is mainly dependent on controlling beam trajectory and emittance dilution from both dispersive plus chromatic effects and wakefield impact. Assuming that a one-to-one trajectory correction scheme is employed to minimize the BPM readings at every quadrupole magnet, the emittance dilution due to dispersive effects is shown below, given a constant relative energy spread $\frac{\sigma_e}{E}$ and a periodic FODO lattice with same focusing in horizontal and vertical plane [17].

$$\Delta\gamma\epsilon_{dis} \approx 4 < y_{BPM}^2 > \sigma_e^2 \frac{\tan\frac{\psi_c}{2}}{L_{cell}^2} \frac{1}{G} \left[{\gamma_f}^2 - {\gamma_i}^2\right] \tag{1}$$

where $\Delta\gamma\epsilon_{dis}$ denotes emittance dilution due to dispersive effects, $< y_{BPM}^2 >$ square of RMS BPM offset (relative to quadrupole), σ_e RMS energy spread of the beam, ψ_c betatron phase advance per FODO cell, L_{cell} FODO cell length, G acceleration gradient, γ_i initial relativistic beam energy and γ_f final relativistic beam energy. One observes that under a similar emittance dilution budget, X-band linac could adopt a shorter cell length for a given betatron phase advance per cell, as it provides a larger acceleration gradient. This also means that the average beta function could be smaller in an X-band linac, in comparison with an S-band linac. On the other hand, for a given FODO cell length L_{cell} one needs a larger average beta function to keep $\tan\frac{\psi_c}{2}$ small.

Considering the accelerator structure misalignment errors which are random about a smoothed trajectory but systematic between a pair of quadrupole magnets, the emittance dilution due to transverse wakefields can be estimated as shown below [17].

$$\Delta\gamma\epsilon_{wake} \approx < y_a^2 > \left[\pi\epsilon_0 N_e r_e \cdot W_\perp(2\sigma_z)\right]^2 \frac{L_{cell}^2}{G \cdot \sin\psi_c} \ln\left(\frac{\gamma_f}{\gamma_i}\right) \tag{2}$$

where $\Delta\gamma\epsilon_{wake}$ denotes emittance dilution due to transverse wakefields, $< y_a^2 >$ square of RMS accelerator structure offset, N_e number of electrons per bunch, $W_\perp$ transverse wake potential. As the transverse wake potential $W_\perp$ is inversely proportional to the fourth power of the cavity iris radius, it is much stronger in an X-band linac than an S-band linac. One then needs to adopt a shorter cell length L_{cell} and a smaller average beta function $\bar{\beta} = \frac{L_{cell}}{\sin\psi_c}$, in order to maintain a smaller emittance dilution $\Delta\gamma\epsilon_{wake}$ from wakefield impacts.

The final choice of the average beta function in the linac should be a balance between controlling emittance dilution from dispersive effects and transverse wakefields. Taking an analytical estimation by using the above two formulae and the associated accelerator parameters, assuming $\sigma_{y_{BPM}} = \sigma_{y_a} = 200\mu m$, one finds that here dispersive effects dominate the transverse emittance dilution, given a relatively large energy spread and a very low electron bunch charge of 10 pC. If real balance on emittance dilution is taken as $\Delta\gamma\epsilon_{dis} = \Delta\gamma\epsilon_{wake}$, one finds that it ends up with very large beta functions which is not realistic. This conclusion is also confirmed by the numerical simulation results shown in the following sections. A relatively long FODO cell length or quadrupole spacing should be adopted here to suppress the possible dispersive emittance dilution.

Another consideration here is to employ fewer quadrupole magnets in all three linacs of this compact FEL driver which decrease the total cost. Based on all the above considerations, the

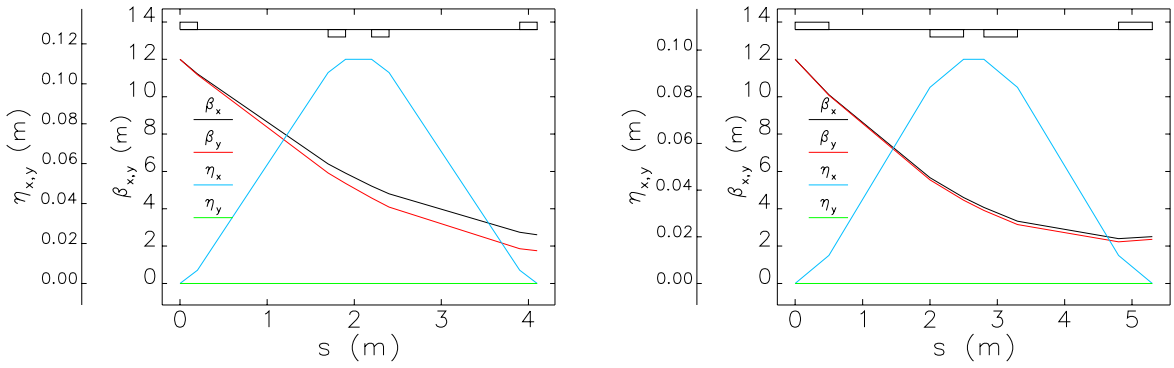

Figure 3: Beta functions and dispersion functions in the bunch compressors. Left: bunch compressor one with a total length of 4 meters, where 0.2-meter-long dipole magnets are employed; Right: bunch compressor two with a length of 5 meters, where 0.4-meter-long dipole magnets are employed. Black curve: horizontal beta function; red curve: vertical beta function; blue curve: horizontal dispersion function; green curve: horizontal angular dispersion function. The transverse optics is quite similar in these two bunch compressors, with the beta function decreasing from 12 meters to 2 meters in the bunch compressor, which is designed to minimize the CSR induced transverse emittance growth.

quadrupole spacing is chosen to be 5 meters in Linac2 and 10 meters in Linac3, which gives an average beta function of roughly 10 meters and 20 meters, respectively. It is a relatively weak focusing structure, where the energy normalized quadrupole strength equals $K_1 = \frac{dB_y}{dx}\frac{1}{B\rho} = 1.2$ in Linac2. In Linac3 the quadrupole strength is even weaker, which is $K_1 = 0.6$. In comparison, an average beta function of 30 to 40 meters is employed in LCLS S-band RF linac. The quadrupole length is chosen to be 0.15 meter in both Linac2 and Linac3, with a total quadrupole number of 18 in all. The associated quadrupole pole tip field ranges roughly from 0.2 kG to 1 kG, with a beam energy from 250 MeV to 6 GeV. It should be easier to achieve a good field quality given a low quadrupole pole tip field employed here.

A laser heater is installed in Linac1 before bunch compressor one, to introduce roughly 2.5 keV un-correlated energy spread, which helps to provide enough Landau damping and suppress collective effects such as longitudinal space charge effects in the overall linac. The length of Linac1 is 5 meters which accelerates the electron bunch from 54 MeV to 250 MeV, on an off-crest RF phase of -15 degree.

Both bunch compressors are designed employing a simple four dipole chicane, with a total length of 4-5 meters. For bunch compressor one at 250 MeV, the dipole length is 0.2 meters and the first order longitudinal dispersion is $R_{56} = -14$ mm. A bunch compression ratio of 7 is achieved in this first stage, which is a reasonable value in maintaining a quasi linear bunch compression process [9]. Linac2 operates at an RF phase of -20 degree, boosts the beam energy to roughly 1.5 GeV, with a correlated energy spread of 0.085 %. Bunch compressor two employs even weaker dipole magnets than bunch compressor one, resulting in a first order longitudinal dispersion of $R_{56} = -8$ mm. One needs to note that the dipole magnet length is increased from 0.2 meters to 0.4 meters, in order to minimize the ISR and CSR impacts on the transverse emittance.

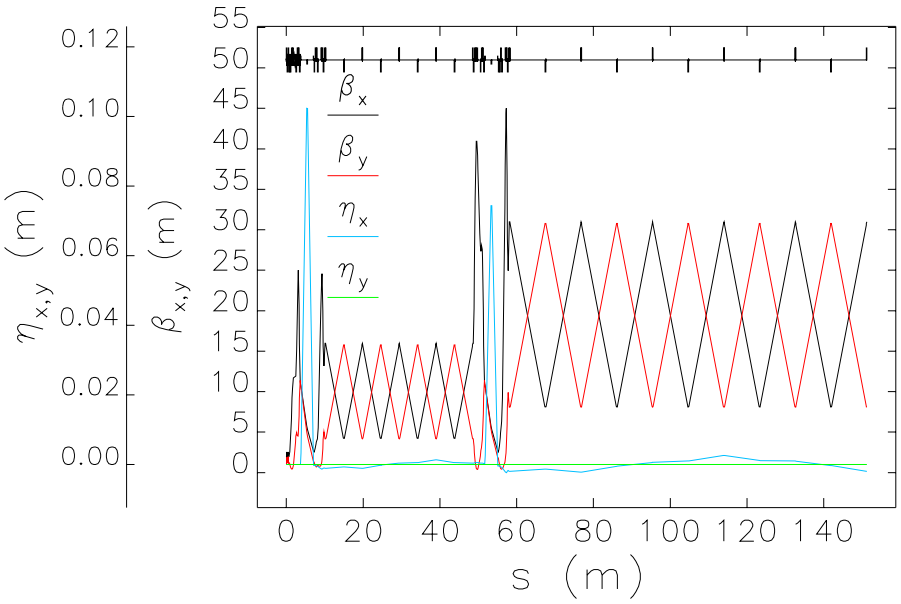

Figure 4: Beta functions and dispersion functions of the overall accelerator, from Linac0 (in Fig. 1) end with an electron beam energy of 54 MeV to linac end with a beam energy of 6 GeV. Black curve: horizontal beta function; red curve: vertical beta function; blue curve: horizontal dispersion function; green curve: horizontal angular dispersion function. Periodic FODO cells are employed for the X-band RF cavity based linac, with an average beta function of 10 meters and 20 meters in Linac2 and Linac3, respectively. Simple matching sections are also employed between linac periodic cell and bunch compressors. The first stage bunch compressor is located at a place where the beam energy is 250 MeV, while the second stage bunch compressor is at 1.5 GeV.

The TWISS parameters of the bunch compressor are designed in such a way that the overall impact from CSR on the horizontal emittance growth is minimized. Basically the horizontal beta function should decrease when the bunch length decreases, and it achieves a minimum at the end of the bunch compressor, as shown in Fig. 3. These optimization methods have experimentally been proven effective in LCLS case [7]. The transverse optics design is similar for both bunch compressors.

There is one matching section at each end of the bunch compressor, which is composed of several quadrupoles and matches the TWISS parameters between linacs and bunch compressors. The electron bunch is running on-crest in Linac3, and the correlated energy offset established in previous linacs is removed by strong longitudinal wakefield of X-band RF cavities. The length of Linac3 is 90 meters, and the beam energy is pushed up to 6 GeV at the linac end, for a hard X-ray FEL radiation at 0.15 nm. The start-to-end linear optics is shown in Fig. 4, for a beam energy boosted from 54 MeV to 6 GeV. The maximum beta function exists in the matching section from linac to each bunch compressor, which is roughly 45 meters.

3.2 X-band wakefield

An analytical formula of the longitudinal point charge wake potential for linac accelerating structure was given by K. Bane [18]. This function, when convolved with a bunch distribution, gives the wake induced by a bunch as shown below. The point charge wake is

$$W_L(s) \approx \frac{Z_0 c}{\pi a^2}\phi(s)\exp\left(-\sqrt{\frac{s}{s_{00}}}\right) \tag{3}$$

where Z_0 denotes vacuum impedance, c speed of light, a iris radius, $\phi(s)$ a step function ($\phi(s) = 1$ for $s > 0$, and $\phi(s) = 0$ for $s < 0$);

$$s_{00} = 0.41 \cdot \frac{a^{1.8} g^{1.6}}{L^{2.4}} \tag{4}$$

where g denotes the gap, L the RF period length.

Similarly, an asymptotic short-range solution is achieved with the fitting method, and the single bunch transverse point charge wake potential is then expressed as shown below [18].

$$W_x(s) \approx \frac{4 Z_0 c s_0}{\pi a^4}\phi(s)\left[1 - \left(1 + \sqrt{\frac{s}{s_0}}\right) \cdot \exp\left(-\sqrt{\frac{s}{s_0}}\right)\right] \tag{5}$$

$$s_0 = 0.169 \cdot \frac{a^{1.79} g^{0.38}}{L^{1.17}} \tag{6}$$

Using these formulae, plus the NLC/GLC H75 X-band structure (SLAC internal ref. name) parameters, both longitudinal and transverse X-band wakefield data files are generated in the Elegant [19] format (SDDS format). A very small longitudinal slice length of 0.01 μm is employed to improve the precision of the wakefield calculation, given an ultra short final bunch length around 0.3 μm.

Both the transverse and longitudinal wakefield strength are stronger for X-band structures, due to their smaller apertures, in comparison with lower frequency RF structures such as S-band or L-band. Employed as an FEL driver, the possible advantage of X-band longitudinal wakefield is that it is more efficient in manipulation of the electron beam's longitudinal phase space, such as cancelling the timing jitter induced bunch length (peak current) variation in Linac2, and removing residual energy correlation in Linac3 where acceleration off-crest has a negligible effect as the final bunch length is too short. Possible disadvantage is that it requires a very precise alignment of the accelerator components and control (steering) of the electron beam's trajectory.

For this FEL design, first the optics of the linac are optimized to suppress the possible impact on transverse emittance growth from the strong X-band structure wakefield. Then transverse emittance dilution is evaluated by simulation where 100 seeds of random misalignment errors are adopted. Here it is also noted that proper steering technique, such as one-to-one steering or dispersion free steering, should be adopted to control the beam trajectory and suppress the transverse emittance growth. Good steering is also necessary in achieving the required final bunch length and peak current. The details will be discussed in Sec. 3.5.

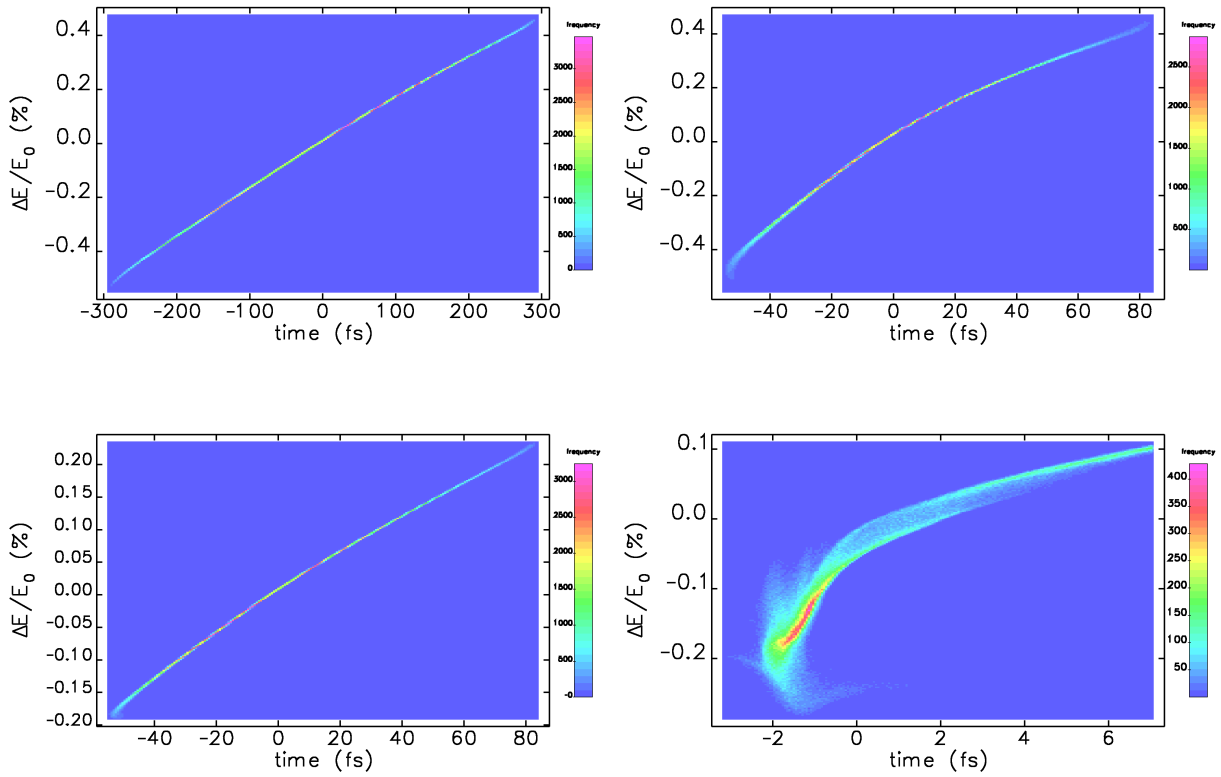

Figure 5: Longitudinal phase space evolution during the acceleration and bunch compression process. Observing locations from left top, right top to left bottom and right bottom: Linac1 end; bunch compressor one end; Linac2 end; bunch compressor two end. The RMS electron bunch length is under-compressed from 140 fs to 34 fs in a first stage bunch compression, then further under-compressed to 2 fs in a second stage bunch compression.

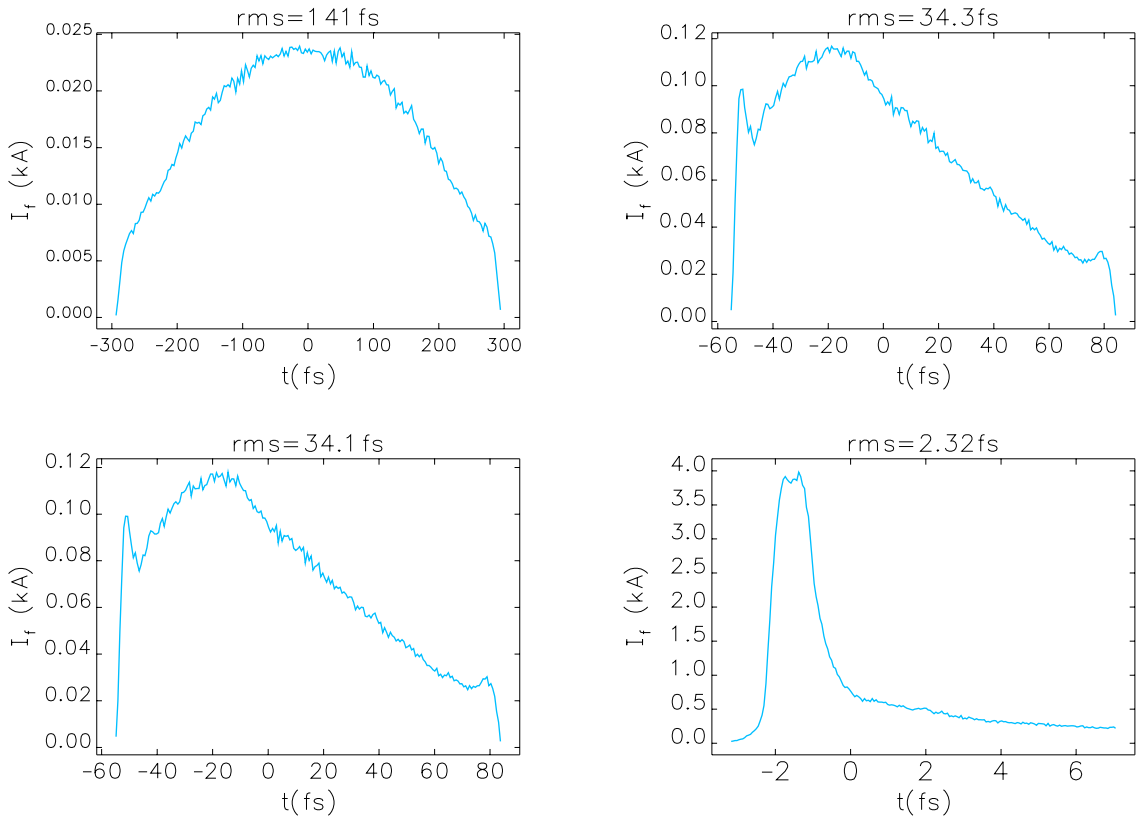

Figure 6: Current profile evolution during the acceleration and bunch compression process. Observing locations from left top, right top to left bottom and right bottom: Linac1 end; bunch compressor one end; Linac2 end; bunch compressor two end. The RMS electron bunch length is under-compressed from 140 fs to 34 fs in a first stage bunch compression, then further under-compressed to 2 fs in a second stage bunch compression.

3.3 Elegant simulation

The designed optics is translated from MAD8 [16] format to Elegant [19] format where a real 3-D simulation is performed with half a million macro particles. As mentioned above, the initial bunch distribution is taken from an output of ASTRA simulation. Longitudinal space charge (LSC) effects is included in all the drift spaces, as well as CSR (1D model in Elegant) and ISR effects in the bunch compressors. Both longitudinal and transverse wakefield effects are included in all the RF cavity elements where an average 'real estate' acceleration gradient of 60 MV/m is adopted, and steering of the beam with random misalignment errors is discussed in next subsection. The longitudinal space charge effect is also included in the drift spaces of all the linac sections.

The initial bunch from ASTRA simulation at 54 MeV has an RMS bunch length of 140 fs and a bunch charge of 10 pC, with a normalized transverse emittance of 0.14 μm in both planes. With the energy modulation established in Linac1 along the longitudinal direction, the bunch length is compressed (under compression) to an RMS value of 30 fs at the exit of bunch compressor one. The bunch is further accelerated from 250 MeV to 1.5 GeV, on an RF phase of -20 degree. The electron bunch length is then further compressed (under compression) to an RMS value of 0.6 fs and an FWHM value of 1.2 fs in bunch compressor two.

The subsequent bunch longitudinal phase space and bunch current profile evolution during the acceleration and compression process is shown in Fig. 5 and Fig. 6, from Linac1 end to Linac2 end. One observes that in Linac1, a quasi linear energy correlation is established by running on an RF phase of -15 degree, with a relatively short electron bunch length of 42 μm. After the electron bunch is compressed to an RMS length of 10 μm in bunch compressor one, the longitudinal phase space tends to be more nonlinear, partially due to the high order dispersions in bunch compressor one and the nonlinear chirp established in Linac1. Then after further acceleration in Linac2 on an RF phase of -20 degree, these nonlinear energy chirps are largely diminished by adiabatic damping and the longitudinal phase space is quasi linear again, as shown in the third subplot of Fig. 5 and Fig. 6. In bunch compressor two, the electron bunch length is further compressed to an RMS value of 0.4 μm, with a peak current over 3 kA. Meantime, at the end of Linac2, a quasi linear residual energy correlation is left on the electron bunch, such that the electron bunch head has a lower energy than its tail, as shown in the fourth subplot of Fig. 5 and Fig. 6.

Coherent Synchrotron Radiation (CSR) effects change particle's energy in the bunch compressor which is a dispersive region, thus it changes the slice trajectory and then increases the projected horizontal emittance of the electron bunch. As mentioned above, LCLS experience [7] is taken here to minimize the impact from CSR effect on the horizontal emittance, which is quite effective. Another point is to do under-compression in both stages and keep the electron bunch away from the full compression state. Here the longitudinally sliced emittance is preserved during the acceleration and both stages of bunch compression, in the core part of the electron bunch. The normalized horizontal emittance does increase to 0.25 μm in the tail of the electron bunch, although this part only represents a very small portion of the beam. The last point is that as the CSR effect is proportional to bunch charge, its impact on electron's energy is relatively small here as a very low bunch charge of 10 pC is adopted. In comparison for a high bunch charge of 250 pC the CSR impact on the emittance growth could be much larger and more difficult to suppress.

The main function of Linac3 is to boost the beam energy to 6 GeV and remove the correlated energy offset which is generated in previous linac for bunch compression purpose. As the X-band

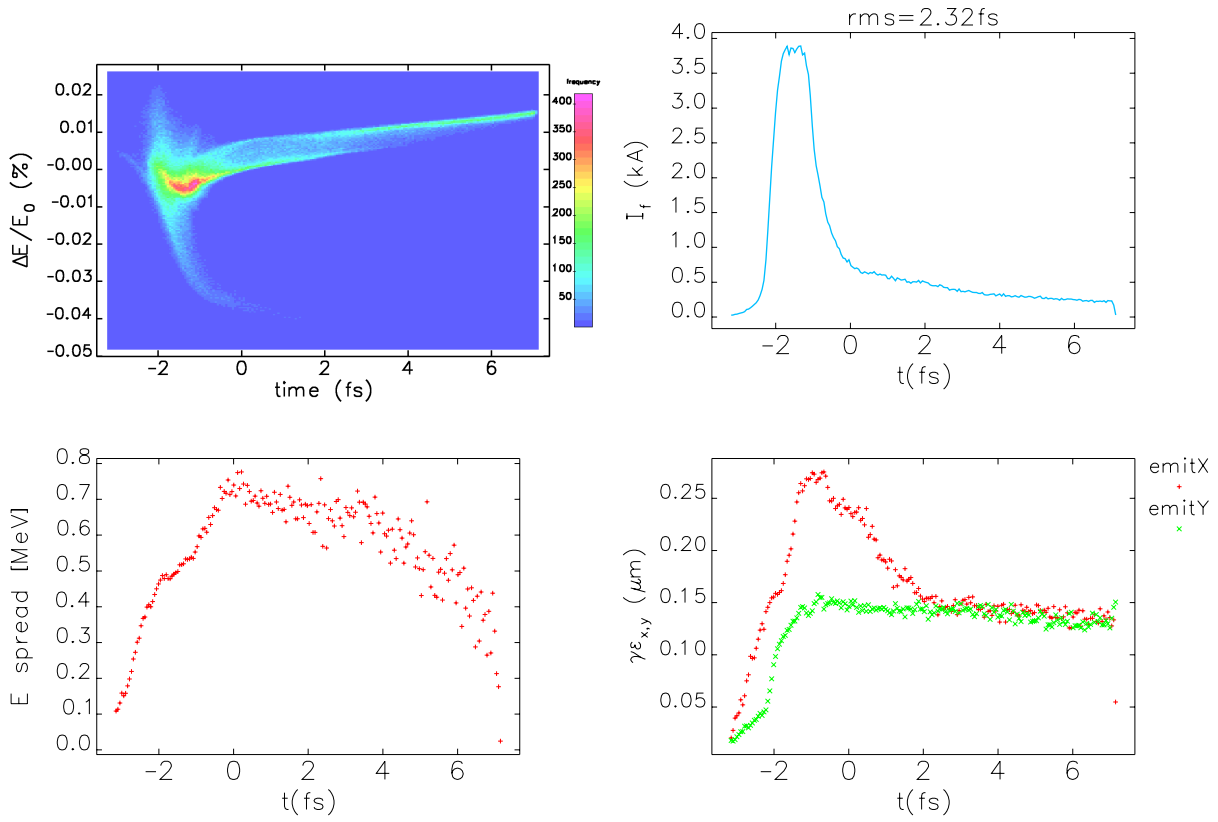

Figure 7: Electron beam properties at the end of Linac3. Left top: longitudinal phase space; left bottom: longitudinally sliced energy spread; right top: current profile; right bottom: longitudinally sliced emittance. A normalized transverse emittance of 0.14 μm is preserved at the core part of the electron bunch, with a pulse duration length of 2 fs. A peak current of 4 kA and a longitudinally sliced relative energy spread less than 1×10^{-4} is achieved. The residual correlated energy offset established in Linac1 and Linac2 is removed in Linac3 with the help of strong X-band RF longitudinal wakefield, and a flat final energy profile is achieved at a beam energy of 6 GeV.

longitudinal wakefield is strong enough and it has an opposite sign in energy chirp with respect to the RF induced energy correlation, it is possible to remove the energy correlation by using only the wakefields in a reasonable length. Another point is that as the final bunch length is very short which is in the femtosecond scale, it is not so effective to generate an energy offset (chirp) using RF acceleration off-crest, even for X-band RF system. Here Linac3 length is chosen to be 90 meters which is long enough to generate the required energy correlation from longitudinal wakefield.

The final beam properties at Linac3 end which is also the undulator entrance are shown in Fig. 7. A flat energy profile is achieved as can be observed in the longitudinal phase space plot. The longitudinally sliced energy spread is less than 1×10^{-4} at a beam energy of 6 GeV, while the longitudinally sliced horizontal normalized emittance is around 0.16 μm, both measured for the core part of the bunch. A peak electron bunch current of 4 kA is produced with a pulse length of 2 fs. A high peak current and small transverse emittance is essential to achieve a short gain length, which in turn shortens the FEL saturation length. A small energy spread along the bunch helps to achieve a small bandwidth of the radiation.

3.4 Timing jitter

In general, an FEL lasing and saturation condition requires a very bright electron beam with a high peak current and a small 3-D normalized emittance. The stability of the final beam current depends on timing and RF phase jitter, also on bunch compressor parameters and electron bunch charge variations. Gun laser to linac RF timing jitter (refered to as timing jitter in the following sections) is considered to be correlated for all the linac sections, which is the main timing error to be discussed in this paper, as the sum of the un-correlated (random) RF phase jitter (different from RF source to source) tends to be small.

There is also a limit on the final electron beam energy variation as the FEL lasing wavelength is inversely proportional to the square of the final beam energy. The beam energy deviation in the linac section and in the bunch compressors is from RF acceleration gradient errors and RF phase errors, while it is also dependent on the timing jitter between gun laser and linac RF system. The difference between this all X-band based FEL and LCLS (S-band RF based) is relatively small given similar feedback loops running. The details of beam energy and bunch charge variations are not discussed in this paper, and only estimations are given on the deterioration in FEL performance.

According to LCLS experiences, a tolerance of 0.1 % relative final electron energy and a 12 % peak current variation need to be met, in order to achieve a successful FEL operation [7]. The tolerance on the initial bunch charge is -6% given a peak current variation of -12 %. Given the LCLS achieved S-Band gun laser stability which provides a charge variation of 1.1%, in this X-Band system a charge variation of 4% is anticipated in the pessimistic sense, considering the gun laser properties and cathode quantum efficiency. The charge variation of 4% in turn would increase the FEL power gain length (and saturation length) by 2.5%, and decrease the output FEL saturation power by 6%, which are estimated under SASE 1D theory.

The achievable charge stability depends on gun laser properties, cathode quantum efficiency and chosen phase with respect to zero-crossing (which is quite different between various X-Band guns, such as the 5.59 cell X-Band gun and the 5.5 cell version), which will be measured experimentally on various X-Band guns.

As there are four times difference in RF frequency and RF wavelength, between S-band RF and

X-band RF, a same timing jitter measured in absolute time would have a much larger impact on this X-band RF based FEL. For a low charge operation mode, such as 10 pC proposed here, its initial bunch peak current is lower if compared with a high charge mode (such as 250 pC). That means one needs to compress more in the electron bunch length, in order to achieve a similar final peak bunch current such as 3 kA. Illustrated by the bunch length variation formula below which is based on a linear model in a single bunch compression stage [20], a large bunch compression ratio implies a tighter tolerance on the timing jitter between photoinjector laser and linac RF system.

$$\frac{\Delta\sigma_{zf}}{\sigma_{zf}} = -\frac{\Delta C}{C_0} = (C_0 \mp 1)\Delta\phi_{rf}\cot\phi_{rf} \approx C_0\frac{\Delta\phi_{rf}}{\phi_{rf}} \tag{7}$$

where $\Delta\phi_{rf}$ denotes timing jitter between photoinjector laser phase and linac RF phase, ϕ_{rf} design linac RF phase (with respect to crest), $\Delta\sigma_{zf}$ change in RMS bunch length, σ_{zf} design bunch length after one stage compression, and C_0 design compression ratio.

However, one also observes from the above formula that choosing a large RF phase ϕ_{rf} makes the relative change in bunch length $\Delta\sigma_{zf}/\sigma_{zf}$ smaller. The bunch charge error also impacts the variation of final peak bunch current, which is not discussed here as it has little connection with RF frequency. Elegant [19] simulations are performed with timing jitter set on all linac RF phase up to 50 fs which is successfully achieved in LCLS operation [7]. This timing jitter of 50 fs changes the Linac1 RF phase and in turn changes the electron bunch length at the end of bunch compressor one. The final relative RMS bunch length variation is around 20 % with 35 meters long Linac2, given a timing jitter of 50 fs between laser and linac RF. One needs to either improve the timing system and achieve a timing error roughly below 25 fs, or find other techniques to cancel the timing jitter effects, to meet the 12% peak current variation upper limit.

Under SASE 1D theory, given an FEL radiation wavelength of 0.15 nm and other beam parameters as discussed above, a timing jitter of 50 fs between laser and linac RF would increase the FEL power gain length (and saturation length accordingly) by 7%. The output FEL saturation power is then 92.8% of the design power.

For this FEL accelerator design, a rising RF slope is employed for bunch compression systems with normal four dipole chicane, where electron bunch head has a lower energy than its tail. In that case, the longitudinal wakefield induced energy chirp always has an opposite sign with the linac RF induced energy chirp. So the longitudinal wakefield in Linac2 can be used to partially or fully cancel the timing jitter induced bunch length variation [7] [21], and generate a more constant final electron current profile. A final electron bunch length at the end of BC2 is then expressed as shown below [21], with timing jitter and wakefield effects considered up to first order. The RF phase ϕ_1 and ϕ_2 denote the ones that has wakefield induced energy chirp subtracted.

$$\sigma_{z2} = \left[1 - k_2(\phi_2 + \Delta\phi_2 - D(\sigma_{z1}, k_2)\cdot L_{Linac2})R_{56(2)}\right]\cdot\left[1 - k_1(\phi_1 + \Delta\phi_1)R_{56(1)}\right]\cdot\sigma_{z0} \tag{8}$$

where $D(\sigma_{z1}, k_2)$ denotes the unit-length change of wakefield induced energy chirp in Linac2 which is a function of RF structure (frequency) and electron bunch length in Linac2, k_1 and k_2 the RF wave number in Linac1 and Linac2, and L_{Linac2} the length of Linac2. In general, the timing jitter induced change on bunch compression ratio (in BC1 and BC2) is compensated by longitudinal wakefield induced energy correlation (chirp) in Linac2. In Linac1 the longitudinal wakefield is weak

as Linac1 has a short length, also one could adopt a Linac1 RF phase with longitudinal wakefield induced energy chirp subtracted. In Linac3 the timing jitter only introduces slight energy variation.

Based on these arguments, one then can decrease the acceleration gradient in Linac2 and increase the Linac2 length (employing more RF cavities), keep the same beam energy at bunch compressor two, and employ a stronger longitudinal wakefield in Linac2 to cancel the timing jitter effect. However, a longer total accelerator length and a higher total cost are accompanied with increasing Linac2 length and employing more RF cavities. A tradeoff needs to be made between the factors mentioned above and the tolerated timing jitter. Analytical and numerical studies show that decreasing the average acceleration gradient from 80 MV/m to 65 MV/m in Linac2 could drop the final peak current variation to 12%. The timing jitter induced peak current variation could be fully compensated if an average acceleration gradient of 50 MV/m is adopted in Linac2. The parameters used in the study are optimum to achieve a shortest accelerator length and a lowest cost, which still provide an acceptable FEL performance.

3.5 Misalignment

In general, the misalignment of the RF structure and quadrupole magnets has two consequences. First, the misalignment of quadrupoles introduces additional dipole kicks on the electron beam, which in turn generates net dispersion. Given a relatively large energy spread in the FEL driver, this introduces dispersive emittance dilution with quadrupole misalignment. Second, the possible misalignment of X-band RF structure makes the electron beam generate stronger transverse wakefield kicks (than S-band RF or other low frequency RF system), which also introduces emittance dilution. As mentioned above, the X-band RF structure has a much smaller radius and then has much stronger transverse wakefield, when compared with L-band or S-band RF structures. Transverse wakefield can imply a longitudinal-position-dependent transverse kick on the electron beam, and then increase the projected emittance.

Here, the transverse wakefield effects are preliminarily evaluated in Elegant simulation where 100k macro particles are employed. First, an RMS value of 20 μm is adopted for the random offset of all the quadrupoles and RF structures in both horizontal and vertical plane. No steering on the electron beam is employed and in that case the transverse emittance dilution is still negligible, compared with the perfect case where there is only emittance growth in the bending plane (mainly due to CSR effects). This small projected emittance growth is dominated by the energy spread related dispersive and chromatic emittance dilution, and the transverse wakefield has a negligible effect. The final bunch length and peak current is not changed. These simulation results show that the linac optics is weak enough in betatron focusing to suppress dispersive and chromatic emittance dilution. Another point is that the linac length is relatively short which has only 10 FODO cells in all.

Next, horizontal and vertical offsets with an RMS value of 200 μm is generated randomly for all the quadrupoles and RF structures in the linac, while an RMS value of 200 μm is assumed for the offset between BPM (Beam Position Monitor) electrical center and quadrupole magnetic center. It is noted that these numbers of 200 μm are assumed in a reasonable manner, which are on a similar level of future linear colliders. In the FEL accelerator optics, there are one BPM and one steering corrector attached on each quadrupole, which measures and steers in both horizontal and vertical plane. 100 random seeds are generated for quadrupole (RF structure) offsets and BPM

to quadrupole offsets. For each error seed, either one-to-one steering or dispersion free steering (DFS) [22] is employed to calculate the required corrector strength and then steer the electron beam on a corrected trajectory. As shown in Fig. 8, it is observed that the projected normalized emittance is almost preserved with either steering method applied with only one iteration. For better illustration, in the bunch compressor the dispersion subtracted emittance is used instead of the projected emittance. Again it is observed that the projected emittance dilution from transverse wakefield is negligible, thanks to the very low bunch charge of 10 pC. Most of the transverse emittance growth is due to CSR impacts in the bunch compression process. Another point is that the longitudinally sliced emittance is not affected by the transverse wakefield.

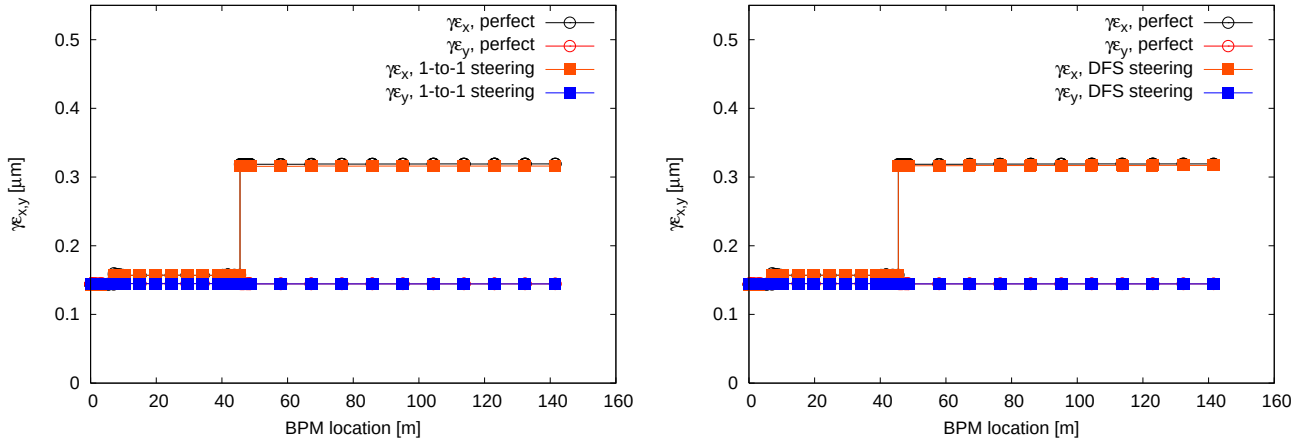

Figure 8: Left: After one iteration of one-to-one steering, dispersive and chromatic emittance dilution (energy spread correlated) is suppressed. Right: After one iteration of dispersion free steering, dispersive and chromatic emittance dilution (energy spread correlated) is suppressed. In the simulation 200 μm (RMS) random offsets are applied on all the quadrupoles and RF structures, and 200 μm is assumed for the offset between BPM (Beam Position Monitor) electrical center and quadrupole magnetic center. The result is an average of 100 random error seeds.

4 Free Electron Laser Performance

The above generated high quality electron bunch is ready to drive a hard X-ray free electron laser (FEL). As mentioned above, in this paper we are studying low charge operation mode (10 pC) with an ultra short photon pulse length of 2-4 fs. The electron bunch distribution generated from ELEGANT simulation is then fed into an undulator system, and the associated FEL performance is simulated and evaluated within the code GENESIS [10].

In the following, we show a concrete example of lasing at 0.15 nm FEL, which wavelength is equivalent as that achieved in LCLS. An ideal undulator is designed to have a short period of $\lambda_w = 1.5$ cm, and the undulator strength K is chosen according to Eq. (9) shown below, with the centroid energy of the electron bunch chosen at 6 GeV, so that the resonant FEL wavelength is $\lambda_r = 0.15$ nm. No nonlinear magnetic field is included for the undulator model. In comparison,

LCLS has to go to a higher beam energy of 14 GeV and then achieve a resonant radiation wavelength of 0.15 nm, as its undulator has a longer period of 3 cm.

$$\lambda_r = \lambda_w \frac{1 + K^2/2}{2\gamma^2}, \tag{9}$$

where γ is the Lorentz factor of the centroid electron energy, and we have assumed a planar undulator. External intersperse FODO focusing lattice is assumed to be implemented for the undulator system, so that the averaged β-function is about 13 m in the undulator.

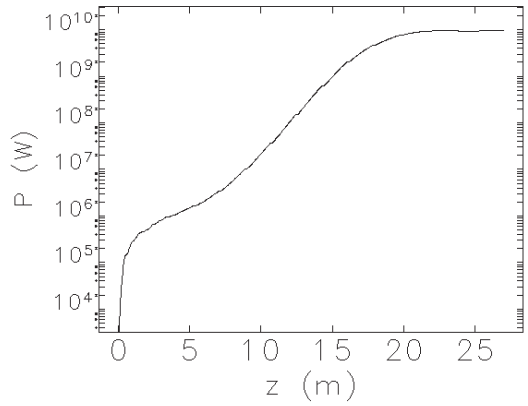

Figure 9: FEL power evolution along the undulator.

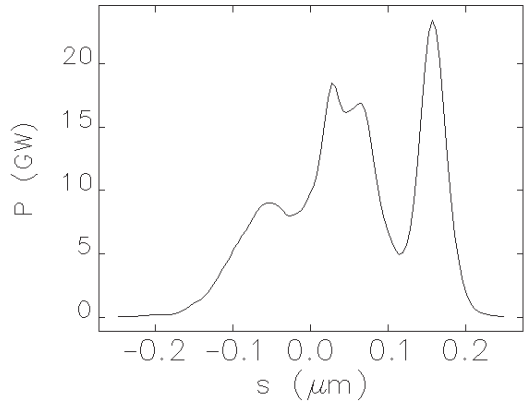

Figure 10: FEL power temporal profile at 20 m into the undulator.

Given such an electron bunch with very small sliced transverse emittance and energy spread, within 20 m long undulator the FEL radiation achieves saturation with a saturation power of $P_{sat} \sim 10$ GW as shown in Fig. 9. In comparison, LCLS has a similar FEL lasing power with a longer saturation length of 60 m. An overall undulator length of 30 m should be enough to

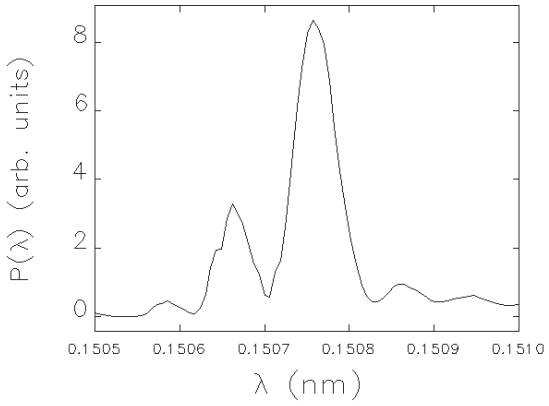

Figure 11: FEL power spectrum at 20 m into the undulator.

achieve saturation. For such a system, the cooperation length of the FEL is about $l_c \sim 0.1$ μm. As mentioned above, the final electron FWHM bunch length is about 0.3 μm as shown in Fig. 7, we expect that the FEL pulse will approach single spike operation mode. Genesis simulation does support this expectation. The temporal profile and the spectral profile of the FEL pulse at 20 m into the undulator are shown in Fig. 10 and Fig. 11, respectively. One sees that the final FEL pulse is reaching single coherent mode in such a low charge scheme.

The radiation wavelength could be tuned in a range of 1.5-0.15 nm, given same undulator configuration, by changing the electron beam energy between 2 GeV and 6 GeV. For a lower beam energy of 2 GeV and a radiation wavelength of 1.5 nm, it should be easier to achieve saturation as the gain length is shorter. As mentioned before, the radiation wavelength, the saturation power and length, as well as the wavelength tunable range is comparable to the low charge mode (20 pC) of LCLS. The number of total photons from a single bunch is only a half of LCLS case, as the bunch charge is a half. One then could employ a higher repetition rate and increase the photon energy per unit time.

5 Conclusion and discussion

A compact hard X-ray FEL design is presented in this paper, which is based on all X-band technology. The total length of this FEL accelerator plus undulator is roughly 180 meters, from X-band photoinjector to the undulator end, which makes it possible to be built given a limited available space. Normal four dipole chicane system is employed as bunch compressors in both stage bunch compression. The optics design of the bunch compressors and linac is optimized to minimize the impacts of CSR, dispersion and wakefields effects. This FEL design is dedicated for a low charge mode operated at 10 pC, with a final photon pulse length of roughly 2 fs. 3-D start-to-end simulations are employed to evaluate the performance of this hard X-ray FEL, using computer codes such as ASTRA, Elegant and Genesis. A final beam current above 3 kA is achieved with a small transverse emittance and small relative energy spread at a beam energy of 6 GeV. To maintain a relatively high average FEL power, higher repetition rate could be employed in this FEL, while a

final pulse length of 2 fs is generated with a bunch charge of 10 pC. In an undulator with a period of $\lambda_w = 1.5$ cm, the compressed electron beam lases successfully at a wavelength of $\lambda_r = 0.15$ nm, and the FEL power saturates at 10 GW over a length of 20 meters. For this low charge operation mode, the FEL pulse approaches to a single coherent spike. The radiation wavelength can be tuned by changing the final electron beam energy. The timing jitter effects between photoinjector laser and linac RF phase are evaluated analytically. It is possible to minimize its impact on the final bunch length (peak current) variation by employing a longer Linac2 with a lower acceleration gradient. Preliminary studies show that the transverse wakefield induced emittance dilution is negligible as a low charge of 10 pC is employed. The additional emittance dilution could be suppressed by one-to-one or dispersion free steering after only one iteration, while the overall emittance growth is mainly due to CSR impacts in bunch compressor two. The performance of this X-band RF driven hard X-ray FEL is equivalent to the low charge mode of LCLS, and it has a shorter accelerator plus undulator length of 180 meters compared with 1230 meters of LCLS accelerator and undulator.

6 Acknowledgement

The authors would like to thank P. Emma, Y. Ding, W. Wan, Z. Huang for helpful discussions. This work was supported by the DOE under Contract DE-AC02-76SF00515.

References

[1] J. Madey, "Stimulated Emission of Bremsstrahlung in a Periodic Magnetic Field," J. Appl. Phys. **42**, 1906 (1971).

[2] D. A. G. Deacon, L. R. Elias, J. M. J. Madey, G. J. Ramian, H. A. Schwettman, and T. I. Smith, "First Operation of a Free-Electron Laser," Phys. Rev. Lett. **38**, 892 (1977).

[3] Ya.S. Derbenev, A.M. Kondratenko, and E.L. Saldin, Nucl. Instrum. Methods Phys. Res. A 193, page 415 (1982).

[4] R. Bonifacio, C. Pellegrini, and L.M. Narducci, Opt. Commun. 50, page 373 (1984).

[5] J.B. Murphy, C. Pellegrini, and R. Bonifacio, Opt. Commun. 53, page 197 (1985).

[6] J. Rossbach, "Results from the VUV-FEL," in Proceedings of the 2006 European Particle Accelerator Conference, p. 34 (2006).

[7] P. Emma *et al.*, Linac Coherent Light Source Conceptual Design Report, SLAC-R-593, SLAC (2002); P. Emma *et al.*, "First lasing and operation of an angstrom-wavelength free-electron laser," Nature Photonics **4**, 641-647 (2010).

[8] TESLA Technical Design Report, TESLA FEL 2002-09, DESY (2002); SPring-8 Compact SASE Source Conceptual Design Report, http://www-xfel.spring8.or.jp (2005); I. S. Ko, in Proceedings of the 2005 Free Electron Laser Conference, p. 216 (Stanford, CA, USA, 2005). PSI SwissFEL design report, www.psi.ch/swissfel/HomeEN (2011).

[9] Yipeng Sun, "Simple limits on achieving a quasi-linear magnetic compression with or without harmonic RF for an FEL driver," SLAC Report No: SLAC-PUB-14445 (2011).

[10] S. Reiche, "GENESIS 1.3: a fully 3D time-dependent FEL simulation code," Nucl. Instrum. Methods A **429**, 243-248 (1999).

[11] C. Limborg-Deprey *et al.*, "An X-band gun test area at SLAC," in Proceedings of the PAC 2011, MOP015 (2011).

[12] A.E. Vlieks, *et al.*, "Recent measurements and plans for the SLAC Compton X-ray source," SLAC-PUB-11689, 10pp., published in AIP Conf.Proc.807:481-490 (2006).

[13] K. Floettmann, ASTRA user manual, http://www.desy.de/mpyflo/Astradokumentation.

[14] O.J. Luiten, S.B. vanderGeer, M.J. deLoos, F.B. Kiewiet, M.J. vanderWiel, "How to Realize Uniform Three-Dimensional Ellipsoidal Electron Bunches," Phys. Rev. Lett. **93**, 094802 (2004).

[15] K.L.F. Bane and P. Emma, "Litrack: A Fast Longitudinal Phase Space Tracking Code with Graphical User Interface," Proceedings of the 2005 Particle Accelerator Conference, 16-20 May 2005, pp. 4266-4268 (2005).

[16] H. Grote, F.C. Iselin, "The MAD Program (Methodical Accelerator Design) Version 8.15," CERN/SL/90-13 (AP) (1990).

[17] T.O. Raubenheimer, "Estimates of emittance dilution and stability in high-energy linear accelerators," Phys. Rev. ST Accel. Beams **3**, 121002 (2000).

[18] K.L.F. Bane, "Short-Range Dipole Wakefields in Accelerating Structures for the NLC," SLAC Report No: SLAC pub-9663 (2003).

[19] M. Borland, "elegant: A Flexible SDDS-Compliant Code for Accelerator Simulation," Advanced Photon Source LS-287, (September 2000).

[20] T. Raubenheimer *et al.*, "Chicane and Wiggler Based Bunch Compressors for Future Linear Colliders," Proc. of PAC'93, Washington, DC (IEEE, Piscataway, NJ, 1993).

[21] Yipeng Sun, Chris Adolphsen and Tor Raubenheimer et al., "Overview of simulation studies on X-band linac driven XFELs at SLAC," SLAC Report No: SLAC-PUB-14471 (2011).

[22] T. Raubenheimer and R. Ruth, "A dispersion-free trajectory correction technique for linear colliders," Nucl. Instrum. Methods A **302**, 191-208 (1991).